

Mode II Fatigue Crack Growth as Influenced by a Compressive Stress Applied Parallel to the Crack Path

A. Otsuka¹, Y. Fujii², K. Maeda² and T. Ogawa³

¹ Professor Emeritus, Nagoya University
B-4, 96-2, Takigawa-cho, Showa-ku, Nagoya 466-0826, Japan
e-mail : aotsuka@sd.starcat.ne.jp

² NTN Corporation, Research & Development Center,
Higashikata 3066, Kuwana 511-8678, Japan
e-mail : yukio_fujii@ntn.co.jp

³ Professor, Department of Mechanical Engineering, Aoyama-gakuin University,
5-10-1 Fuchinobe, Sagamihara 229-8558, Japan
e-mail : ogawa@cc.aoyama.ac.jp

ABSTRACT. *Flaking type failures in rolling contact processes are usually attributed to fatigue-induced subsurface shearing stress caused by the contact loading. Assuming such crack growth is due to mode II loading and that mode I growth is suppressed due to the compressive stress field arising from the contact stress, we developed a new testing apparatus for mode II fatigue crack growth. According to the test results on bearing steel JIS-SUJ2 and other hard steels, stable mode II fatigue crack growth was observed in the range of the values of the ΔK_{II} , namely, between lower bound approximately $3\text{MPa}\sqrt{m}$ and upper bound $5\text{-}10\text{MPa}\sqrt{m}$. The value of upper bound depends on the values of superimposed compressive stress. If applied ΔK_{II} is larger than this critical value, mode I (tensile mode) fatigue crack growth occurs on the plane of maximum tensile stress.*

INTRODUCTION

Flaking type failures in rolling contact fatigue are considered to be initiated and propagated in the material subsurface due to the cyclic shearing stress produced by the contact stress [1]. The contact stress field in the subsurface produces cyclic shearing stresses superimposed on the compressive stress. The flaking type failure mentioned above may therefore be modeled by a crack initiated and propagated by the cyclic shearing stress parallel to the crack together with the superimposed compressive stress. Though the subject of interaction between fracture surfaces is important in the appreciation and application of test results in relation to rolling contact fatigue, we focus in this study on mode II fatigue crack growth characteristics and intrinsic material properties without any effects of fracture surface interactions.

Experimental research on mode II fatigue crack growth has been made on aluminum alloys [2, 3, 4] and on other metals [5, 6] by Otsuka et al. Recently Murakami et al. [7, 8, 9] have developed a new method to obtain mode II fatigue crack growth characteristics which are focused on the ΔK_{II} -threshold of hard steels including SUJ2 [9]. In our present testing method, although the basic idea is the same as the one described in former papers [5, 6], some important alterations have been made relating to the method of

applying mode II loads and the application of a compressive stress.

In the new apparatus, a direct loading system is employed instead of the four-point-shear-loading system used by Gao et al [10] and after Otsuka et al [2, 3, 4]. Though the four-point-shear-loading system has the advantage that a shear loading condition with no bending can be obtained, there are some disadvantages. For example tests under reversed loading are difficult and a rather heavy test structure with large inertia is required. A new device to provide compressive stress to the specimen has now been developed. In the new apparatus a compressive stress is provided by a specially designed jig that employs wedge tightening. In a former apparatus the device to apply compression was integral with the mode II loading system rather than being an independent system. After applying compression to the specimen in our new system, as described above, the combined mode II loading apparatus and the specimen is assembled in the fatigue testing machine. Due to these alterations, the new apparatus is rather compact and mode II cyclic loading tests for hard steels are now possible for arbitrary stress ratios, including fully reversed loading ($R=-1$) which is the case in rolling contact fatigue. Fujii et al. [11] have shown that flaking failure in rolling contact fatigue caused by indentation on mating surface can be explained based on the mode II fatigue crack growth characteristics obtained by using this testing apparatus. In the present report, experimental data from mode II fatigue crack growth tests together with procedures using the new apparatus are described involving specimens of SUJ2 and other steels and aluminum alloys.

SPECIMENS AND MODE II TEST METHOD

Materials and Specimens

The materials used are high carbon chromium bearing steel JIS-SUJ2, 0.75%C steel and carbon steel JIS-S53C. SUJ2-specimens were made from three lots, and we call the specimens from these lots SUJ2-1, SUJ2-2 and SUJ2-3, according to the lot. Their hardness are shown in Table 1. Mode I fatigue tests were made by using compact specimen (CT-specimen) of 25mm width and 5mm thickness. The specimen used for mode II fatigue tests is shown in Fig.1.

Experimental Procedures

The new mode II fatigue testing apparatus consists of two loading frames "A" and "B", as shown in Figs. 2 and 3. The ends of the test specimen shown in Fig. 1, are fixed into the frames by wedges; one end in Frame A, the other end in Frame B. The wedges have the role of providing a compressive stress parallel to the crack which will suppress tensile mode crack growth during mode II loading [5, 6]. The tests are carried out in the following order.

(i) Figure 3 (a) shows the fixing of the specimen in the loading frames "A" and "B" using the specially made clamping jig. By tightening the wedges, the specimen is fixed to the loading frames as shown in Fig. 2. The wedges are tightened by driving the screw connected to the handle shown in the Fig. 3 (a). The compression stress induced by the wedges is monitored via the reading of the four strain gages bonded to the specimen as shown in Fig.1. The difference between the readings of the 4 gages was around 5% and always less than 10%. Figure 4 (b) shows the FEM calculations for the compressive stress induced in the specimen by the compressive forces applied on both sides of the specimen by wedge tightening as indicated in Fig. 4 (a), where compressive

Table 1 Materials and hardness

Material	SUJ2-1 (SAE52100 equivalent)	SUJ2-2 (SAE52100 equivalent)	SUJ2-3 (SAE52100 equivalent)	0.75C Steel	JIS S53C (SAE1050 equivalent)
Hardness (HRC)	59	62	61	61	61

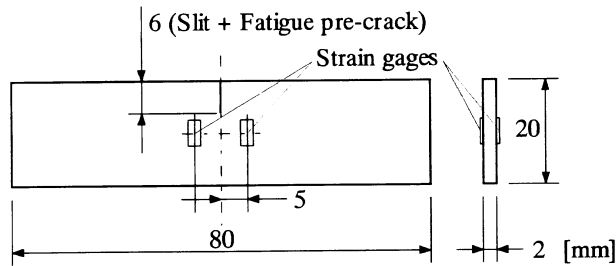


Fig. 1 Mode II specimen .

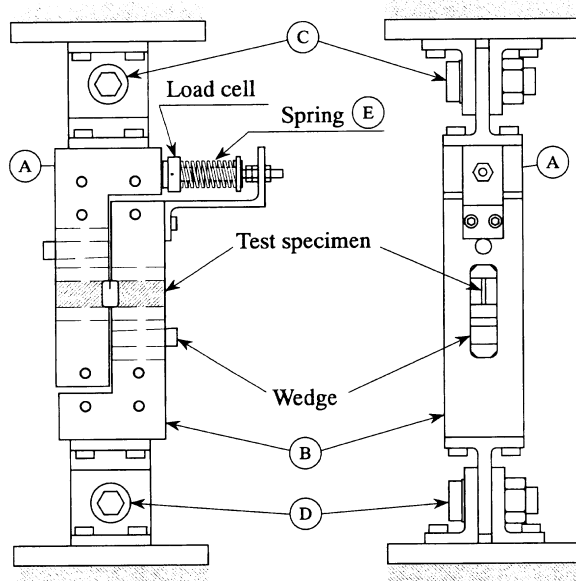


Fig. 2 Test apparatus for mode II fatigue crack growth in a compression stress field.

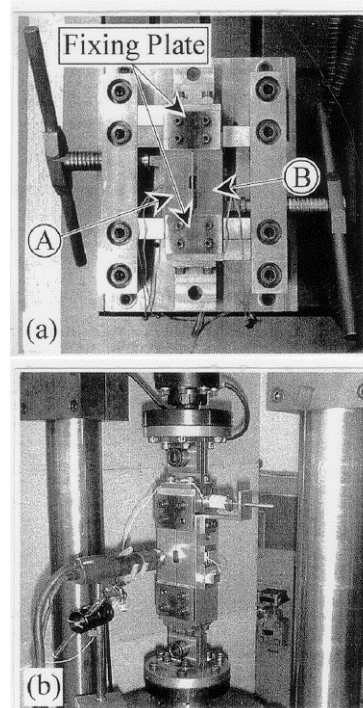


Fig. 3
(a) Fixing of mode II specimen to loading frames "A" and "B", by using the special jig.
(b) Observation of fatigue crack growth with a digital microscope.

stress induced by wedge tightening is assumed to be uniform. According to the results, the compressive stress in the area of fatigue crack growth is around 90% of the value of that recorded by the strain gages.

(ii) After fixing the specimen in the loading frames, the loading frames and the specimen assembly is placed on a horizontal surface plate, and then required amount of K_I is provided by the spring "E" shown in Fig. 2. After that, frames "A" and "B" are fixed by a "fixing plate"(Fig. 3(a)) and bolts. This fixing of frames "A" and "B" by the

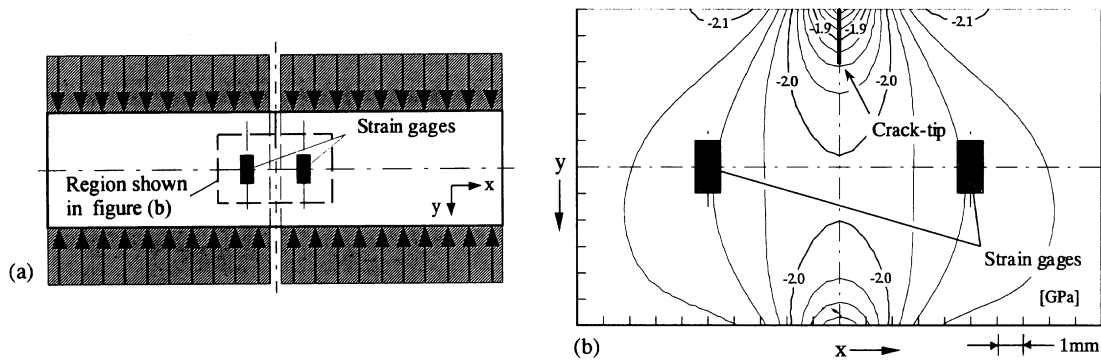


Fig. 4 Compressive stress σ_y induced by the compressive load applied on the both edges of the specimen as shown in the figure. Curves in the figure (b) show the value of σ_y when the applied compressive loads induce a 10 000 compressive micro-strain at the strain gage position shown in the figure (a).

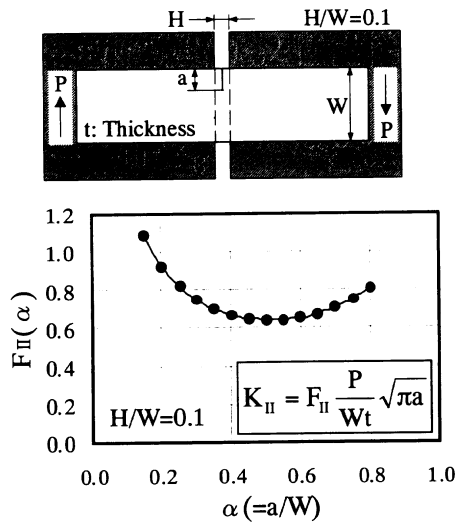


Fig. 5 Values of K_{II} for a single edge-cracked plate with a rigid grip subjected to shear loading.

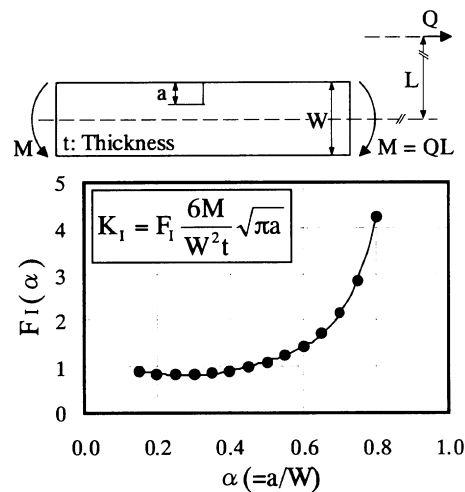


Fig. 6 Values of K_I for a single edge-cracked plate subjected to bending moment.

plate is made so that the specimen will not be subjected to an unexpected load when handling the assembly for the following step (iii).

(iii) Then, the completed assembly of frames "A" and "B" and the specimen, which is clamped by the fixing plate, is mounted on the fatigue testing machine. This mounting is made by tightening the bolts "C" and "D" shown in Fig. 2 to the chucks of the fatigue testing machine.

(iv) The fixing plate is removed and the test may then start. The observation and recording of the fatigue crack during mode II cyclic loading are made with a KEYENCE digital microscope (long distance lens VH-W50, controller VH6100). Figure 3 (b) indicates the positioning and monitoring of the fatigue crack with the digital microscope, while Figure 7 shows examples of recorded results. The calculation of the stress intensity

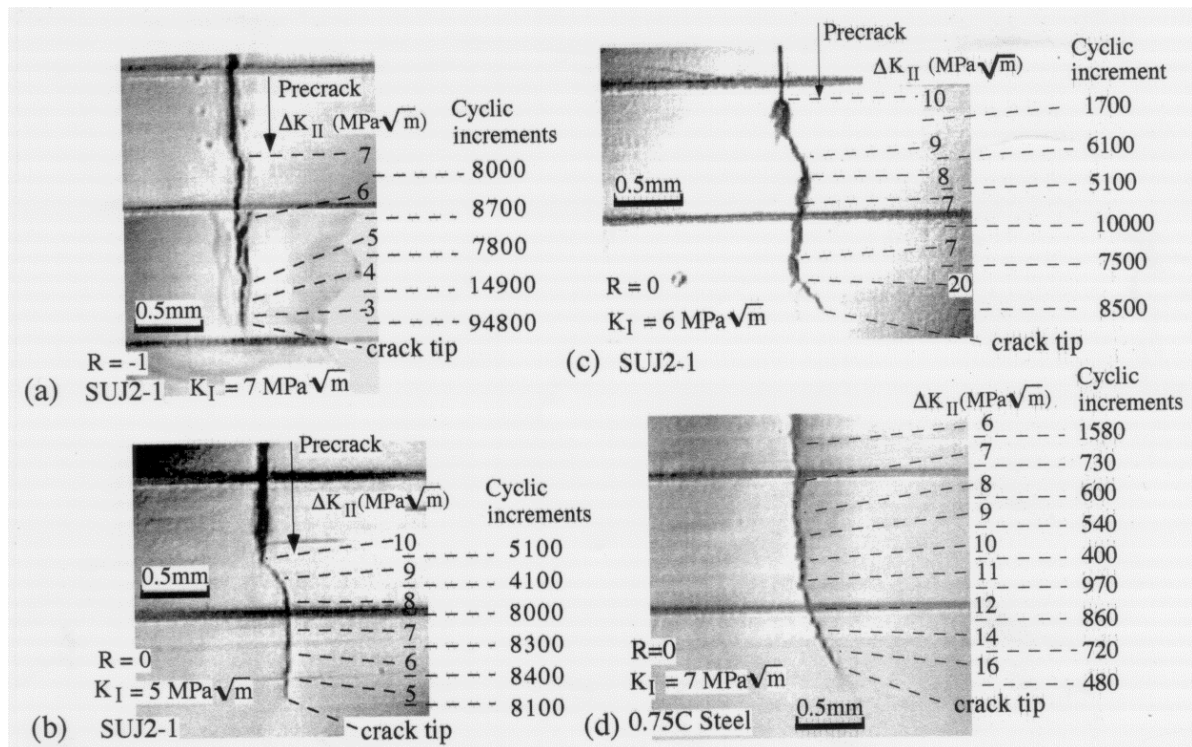


Fig. 7 Fatigue crack growth under mode II loading in SUJ 2 and 0.75C steel specimens. (a) shows mode II fatigue growth in the range of ΔK_{II} smaller than $7 \text{ MPa}\sqrt{\text{m}}$. (b) shows a transition from tensile mode growth in the high ΔK_{II} range to shear mode growth in the low ΔK_{II} range. (c) shows tensile mode growth at the start of crack growth and mode II growth and again tensile mode growth according to the values of applied ΔK_{II} . (d) Transition in fatigue crack growth from mode II growth during low ΔK_{II} to tensile mode growth in high ΔK_{II} range.

factors was made by employing the FEM analysis software MARC (MSC Software Corporation). Figures 5 and 6 show K_{II} values due to the shear loading and K_I due to the bending moment, respectively. [12]

EXPERIMENTAL RESULTS

Fatigue Crack Growth Behavior

Figures 7 (a), (b) and (c) show the fatigue crack growth behavior for SUJ2-1 and Fig.7 (d) shows the behavior for 0.75C steel. These tests were made at, approximately, 10 000 micro-compressive strain measured by strain gages shown in Fig. 1. In the case of Fig. 7 (a), a ΔK_{II} of $7 \text{ MPa}\sqrt{\text{m}}$ was first applied and then the applied ΔK_{II} value was decreased to $3 \text{ MPa}\sqrt{\text{m}}$. The load decreasing was made step by step, as shown in the figure, so as to give the designated ΔK_{II} values at the start of each step. Then the load was kept constant until the next step, at the start of which the load was adjusted again so as to give the next designated value. Figure 7(a) shows that, under the condition that the values of ΔK_{II} are

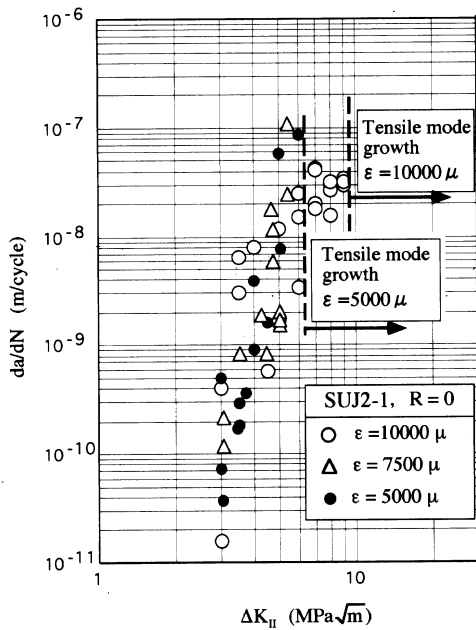


Fig. 8 Effects of compressive stress on mode II fatigue crack growth

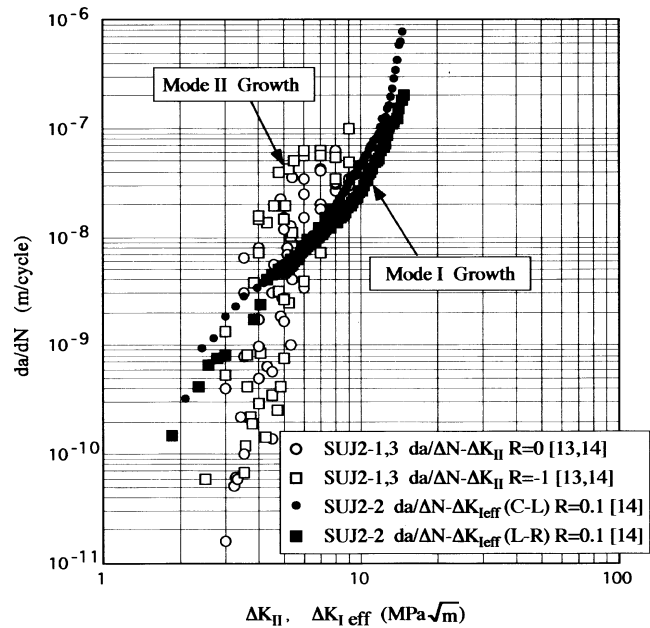


Fig. 9 Mode II fatigue crack growth rate da/dN versus ΔK_{II} relation and mode I fatigue crack growth rate da/dN versus $\Delta K_{I\text{eff}}$ relation for SUJ 2 specimens.

between $7\text{MPa}\sqrt{\text{m}}$ and $3\text{MPa}\sqrt{\text{m}}$, and that the superimposed micro-compressive strain is 10 000, crack growth occurs ahead of the precrack in the direction of the precrack, without showing deflection to tensile mode. In the case of Fig. 7 (b), a ΔK_{II} of $10\text{MPa}\sqrt{\text{m}}$ was first applied and then the applied ΔK_{II} was decreased to $5\text{MPa}\sqrt{\text{m}}$. The results show that fatigue crack growth occurred in the tensile mode initially in the relatively higher ΔK_{II} region and then, with decrease in ΔK_{II} , the direction of crack growth changed gradually and became parallel to the precrack. In the case of Fig. 7 (c), crack growth was initiated in tensile mode and then shows mode II growth in the range between $9\text{MPa}\sqrt{\text{m}}$ and $7\text{MPa}\sqrt{\text{m}}$ and then showed tensile mode growth again when ΔK_{II} was increased to $20\text{MPa}\sqrt{\text{m}}$. In Fig. 7(d), fatigue crack growth occurred in mode II within the range of ΔK_{II} , approximately, between 6 and $10\text{MPa}\sqrt{\text{m}}$, and the crack growth direction changed gradually to the direction of tensile mode growth with an increase of ΔK_{II} .

These test results show that, in the materials tested and under the superimposed micro-compressive strain 10 000, mode II fatigue crack growth occurs in the region where ΔK_{II} is smaller than approximately $9\text{MPa}\sqrt{\text{m}}$. And if we increase the value of ΔK_{II} , transition in the mode of crack growth from mode II (shear mode) to mode I (tensile mode) occurs. The value of ΔK_{II} at which this transition occurs is a function of superimposed compressive stress. Some results related to the effect of compression on mode II-to-mode I transition are shown later in Fig. 8.

$da/dN - \Delta K_{II}$ relations

Figure 8 shows the effects of the compressive stress applied parallel to the crack on mode

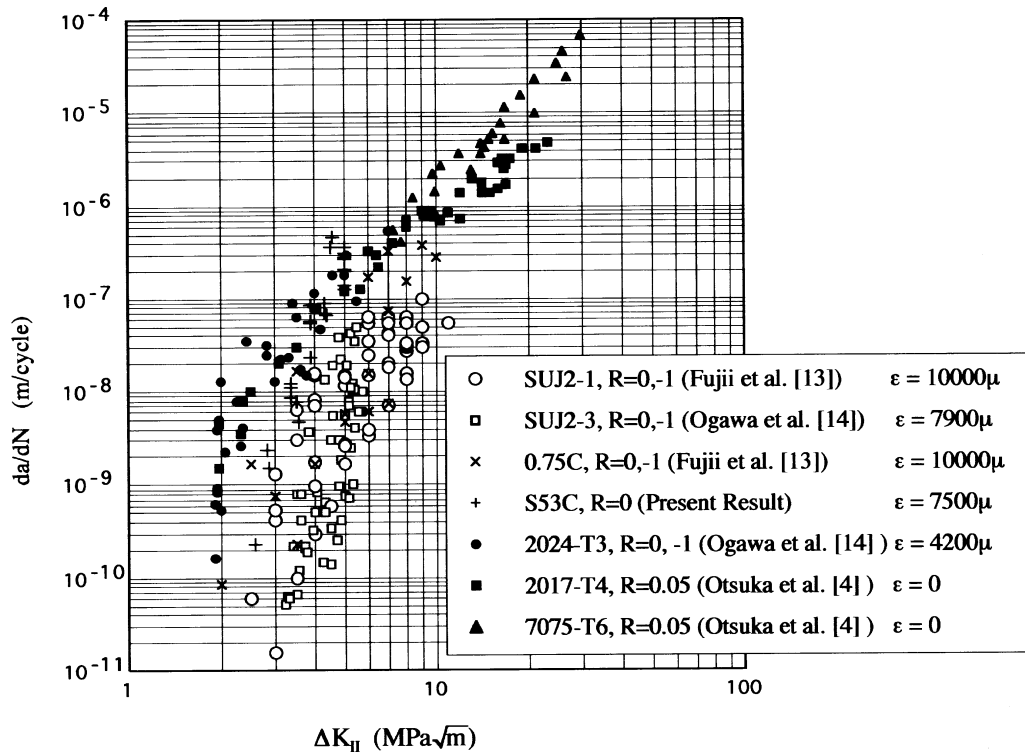


Fig. 10 Mode II fatigue growth rate da/dN versus ΔK_{II} relations for hard steels, SUJ2, 0.75C Steel and S53C; and high strength aluminum alloys, 2024-T3, 2017-T4 and 7075-T6.

II fatigue crack growth. The magnitude of the compressive stress is expressed by the readings of the strain gages (" ϵ " in Figs. 8 and 10) shown in Fig. 1. This figure shows that the magnitude of the compressive stress has almost no effect on da/dN - ΔK_{II} relation and on the threshold values for mode II fatigue crack growth, while it is noticed that the critical value of ΔK_{II} at which mode II (shear mode)-to-mode I (tensile mode) transition occurs is a function of the magnitude of the compressive stress. According to the test results, the transition occurred at around $9\text{MPa}\sqrt{\text{m}}$ when the micro-compressive strain $\epsilon = 10000$ and at around $5\text{MPa}\sqrt{\text{m}}$ when $\epsilon = 5000$.

Figure 9 shows the comparison of da/dN - ΔK_{II} relations for mode II fatigue crack growth with da/dN - $\Delta K_{I\text{eff}}$ relation for mode I fatigue crack growth where mode I tests were made by using CT-specimens and $\Delta K_{I\text{eff}} = K_{I\text{max}} - K_{OP}$. The values of K_{OP} were obtained by the compliance method. Mode II fatigue tests were made at stress ratios $R = 0$ and -1 . This data shows that da/dN in mode II fatigue is determined by the range of ΔK_{II} , regardless of stress ratios at least in the range $R = -1$ and 0 . This figure also shows that ΔK_{II} -dependence of da/dN for mode II fatigue is larger than ΔK_I -dependence for mode I fatigue. It is also shown that the threshold for mode II fatigue crack growth $\Delta K_{II\text{th}}$ is around $3\text{MPa}\sqrt{\text{m}}$ and the threshold value for mode I fatigue $\Delta K_{I\text{eff-th}}$ (the threshold value expressed in effective stress intensity factor range) is around $2\text{MPa}\sqrt{\text{m}}$.

Figure 10 shows the material-dependence of da/dN - ΔK_{II} relations for mode II fatigue crack growth. Materials used for the test are high hardness steels including bearing steel

SUJ2, 0.75%C steel and S53C; and high strength aluminum alloys, 2024-T3, 2017-T4 and 7075-T6. This figure shows that da/dN for carbon steels S53C and 0.75%C steel specimens show higher da/dN than that of bearing steel SUJ2 specimens. This result probably suggests that this mode II fatigue test will be useful for material evaluation for the materials used under the condition of rolling contact fatigue. If we compare da/dN for steels with those of aluminum alloys, it may be suggested that da/dN for mode II growth will be Young's modulus-dependence, as in the case of mode I fatigue crack growth.

CONCLUSIONS

Based on the assumption that flaking type failure in rolling contact fatigue is due to mode II loading and that mode I growth is suppressed due to the compressive stress arising from the contact stress, a new testing apparatus for mode II fatigue crack growth has been developed. Some test results on bearing steel and other materials obtained by using this apparatus have been shown.

REFERENCES

1. T. A. Harris (2001) *Rolling Bearing Analysis*, Fourth edition, John Wiley & Sons, Inc., New York.
2. A. Otsuka, K. Tohgo, T. Kiba and S. Yamada (1984) In: Proc. ICF 6, *Advances in Fracture Research*, vol.3, pp. 1671 - 1678, Pergamon Press.
3. A. Otsuka, K. Tohgo and Carl Erik Skjølstrup (1986) In : *The Mechanism of Fracture*, Metals/Materials Technology Series, pp. 265-275, American Society for Metals.
4. A. Otsuka, K. Mori and K. Tohgo (1987) In: *Current Research on Fatigue Crack*, Current Japanese Materials Research vol.1. pp.149-180, T. Tanaka, M. Jono and K. Komai (Eds.) Elsevier Applied Science, London and New York,
5. A. Otsuka and M. Aoyama, (1993) In: *Mixed-mode Fatigue and Fracture*, pp.49-60, H.P. Rossmannith and K.J. Miller (Eds) Mechanical Engineering Publications. London.
6. A. Otsuka, H. Sugawara and M. Shomura (1996) *Fatigue Frac. Engng. Mater. Struct.*, **19** (10), 1265-1275.
7. Y. Murakami, S. Hamada, S. Kazuno and K. Takao (1994) *J. Soc. Mat. Sci. Japan*, **43** (493), 1264-1270. (in Japanese)
8. Y. Murakami, C. Sakae and S. Hamada (1997) In: *Engineering Against Fatigue*, pp. 473-485, J.H. Beynon , M.W. Brown ,T.C. Lindley , R.A. Smith and B. Tomkins (Eds) Univ. of Sheffield.
9. Y. Murakami, T. Fukuhara and S. Hamada (2002) *J. Soc. Mat. Sci. , Japan*, **51** (8), 918-925. (in Japanese)
10. Gao Hua, M. W. Brown and K.J. Miller (1982) *Fatigue Engng Mater. Struct.*, **5**, 1-17.
11. Y. Fujii and K. Maeda (2002) *Wear*, **252**, 811-823.
12. Y. Murakami (Ed.) (2002), *Stress Intensity Factors Handbook*, Vol. 4, Elsevier Science, 919-920.
13. Y. Fujii, K. Maeda and A. Otsuka (2001) *J. Soc. Mat. Sci., Japan*, **50**, 1108-1113. (in Japanese)
14. T. Ogawa, O. Hirayama and T. Kimoto (2002) *Proceedings of the 26th Symposium on Fatigue*, pp. 41-44, Soc. Mat. Sci., Japan. (in Japanese)